Muscle contributions to tibiofemoral shear forces and valgus and rotational joint moments during single leg drop landing

Maniar, Nirav, Schache, Anthony G., Pizzolato, Claudio and Opar, David A.

Lower-limb muscle force contributions to tibiofemoral shear forces and valgus and rotational joint moments during single leg drop landing

Authors

Nirav Maniar[1] Anthony G Schache[2], Claudio Pizzolato[3, 4], David A Opar[1]

[1] School of Behavioural and Health, Australian Catholic University, Melbourne, Australia

[2] La Trobe Sports and Exercise Medicine Research Centre, La Trobe University, Melbourne, Australia

[3] School of Allied Health Sciences, Griffith University, Australia

[4] Griffith Centre of Biomedical and Rehabilitation Engineering (GCORE), Menzies Health Institute Queensland, Griffith University, Australia.

Corresponding author

Nirav Maniar

Nirav.Maniar@acu.edu.au

+61 3 9953 3742

17 Young Street

Fitzroy, VIC, Australia

3065

Acknowledgements

The authors acknowledge the support provided by the Australian Government Research Training Program Scholarship.

ABSTRACT

Anterior cruciate ligament (ACL) injuries commonly occur during single leg landing tasks and are a burdensome condition. Previous studies indicate that muscle forces play an important role in controlling ligamentous loading, yet these studies have typically used cadaveric models considering only the knee-spanning quadriceps, hamstrings and gastrocnemius muscle groups. Any muscles (including non-knee-spanning muscles) capable of opposing the anterior shear joint reaction force and the valgus joint reaction moment are thought to have the greatest potential for protecting the ACL from injury. Thus, the purpose of this study was to investigate how lower-limb muscles modulate knee joint loading during a single leg drop landing task. An electromyography-informed neuromusculoskeletal modelling approach was used to compute lower-limb muscle force contributions to the anterior shear joint reaction force and the valgus joint reaction moment at the knee during a single leg drop landing task. The average shear joint reaction force ranged from 153N of anterior shear force to 744N of posterior shear force. The muscles that generated the greatest posterior shear force were the soleus, medial hamstrings, and biceps femoris, contributing up to 393N, 359N and 162N, respectively. The average frontal plane joint reaction moment ranged from a 19Nm varus moment to a 6Nm valgus moment. The valgus moment was primarily opposed by the gluteus medius, gluteus minimus and soleus, with these muscles providing contributions of up to 38Nm, 22Nm and 20Nm towards a varus moment, respectively. The findings identify key muscles that mitigate loads on the ACL.

Key terms: anterior cruciate ligament, dynamic valgus, neuromechanics, dynamic coupling, opensim.

INTRODUCTION

Athletes that participate in sports requiring high impact landings and cutting tasks are at risk of anterior cruciate ligament (ACL) injury [1]. The majority of these injuries are treated with surgical intervention [1] resulting in substantial convalescence and rehabilitation time [2] as well as associated financial costs [3]. Moreover, ACL rupture is associated with potential long term consequences, including high re-injury rates (~15%) [4] and the development of knee osteoarthritis later in life [5]. Therefore, prevention of ACL injury is pertinent, and knowledge regarding the mechanical factors related to ACL injury and injury risk is needed to develop effective prophylactic strategies.

ACL rupture occurs when the mechanical load experienced by the ligament exceeds the ligament's ability to withstand that mechanical load. Rupture may be a consequence of a single catastrophic load or the consequence of repetitive cyclic loading leading to microdamage and thus fatigue failure [6]. Irrespective of the circumstance, the relevant mechanical loads at the knee that are considered most likely to cause damage to the ACL are anterior shear forces, valgus moments and internal rotation moments, especially when these loads occur simultaneously [7,8]. It is therefore important to understand how these mechanical loads are developed during key injurious manoeuvres, such as change of direction or single leg landing tasks [9,10]. Such knowledge could be beneficial for improving ACL prevention strategies.

Muscles produce forces that can modulate (i.e., both accentuate and oppose) these critical mechanical loads at the knee. For example, it is known that the quadriceps tends to generate an anterior tibiofemoral shear force which is directly opposed by the ACL, whilst the hamstrings tend to do the opposite [11]. However, the majority of the existing research on this topic has only considered the role of major knee-spanning muscles. Through "dynamic coupling", any muscle in the body can potentially induce an acceleration of any segment in the body [12]. Subsequently, it is possible that certain non-knee-spanning muscles can influence knee joint loads during injurious manoeuvres. For example, our previous work investigating unanticipated sidestep cutting has demonstrated the importance of the soleus for opposing the anterior shear force, and the gluteus medius for opposing the valgus moment [13]. Since the way in which a muscle induces reaction forces is dependent on the kinematics of all segments in the system [12], it is likely that muscle force contributions to knee joint loading is task specific. It may not be appropriate to infer the role of specific muscles from unanticipated sidestep cutting to other key injurious manoeuvres, such as single leg landing.

Therefore, the purpose of this study was to determine which muscles have the greatest potential to oppose (or control) the anterior shear force as well as the valgus and internal rotation moments at the knee during a single leg drop landing task. Specifically, we used an electromyography (EMG) informed neuromusculoskeletal modelling approach to predict lower-limb muscle contributions to the anteroposterior shear joint reaction force as well as the valgus/varus and internal/external rotation joint reaction moments at the knee. Based on prior work [13,14], we hypothesized that the anterior shear force would be primarily opposed by the hamstrings and soleus, whilst the valgus moment would be primarily opposed by the gluteus medius.

MATERIALS AND METHODS

Participants

Eight recreationally active healthy males (age: 27 ± 4 years; height: 1.77 ± 0.09m; mass: 78 ± 13kg) volunteered to participate in this study, which formed part of a larger project investigating high impact dynamic tasks [13,15,16]. All participants had no current or previous musculoskeletal injury likely to influence their ability to perform the required tasks. All participants provided written informed consent to participate in the study. Ethical approval was granted by the Australian Catholic University Human Research Ethics Committee (approval number: 2015-11H)

Instrumentation

Three-dimensional marker trajectories were collected at 200Hz using a nine-camera motion analysis system (VICON, Oxford Metrics Ltd., Oxford, United Kingdom). Ground reaction forces (GRF) were collected via a ground-embedded force plate (Advanced Mechanical Technology Inc., Watertown, MA, USA) sampling at 1000Hz. Surface EMG data were collected at 1000Hz from 10 lower-limb muscles on the dominant leg (defined as the kicking leg; right side for all participants) via two wireless EMG systems (Noraxon, Arizona, USA; Myon, Schwarzenberg, Switzerland).

Procedures

All participants completed the experimental tasks barefoot, which allowed exposure of the foot for marker placement. The skin was prepared for surface EMG collection by shaving, abrasion and sterilisation. Circular bipolar pre-gelled Ag/AgCl electrodes (inter-electrode distance of 2cm) were then placed on the vastus lateralis and medialis, rectus femoris, biceps femoris, medial hamstrings, medial and lateral gastrocnemius, soleus, tibialis anterior and peroneus longus muscles in accordance with Surface Electromyography for the Non-Invasive Assessment of Muscle (SENIAM) guidelines [17]. EMG time traces during forceful isometric contractions were visually examined to verify the correct placement of the electrodes and to inspect for cross-talk. Additionally, participants were required to perform at least two isometric maximum voluntary contraction trials (knee flexion and extension, ankle plantar- and dorsi-flexion) in order to obtain an appropriate reference value to normalise the EMG data. For each of these trials, the investigator provided firm manual resistance against the participant's contraction for the full three-second duration of the repetition (see Supplementary Figure 1 for further details) and provided verbal encouragement to the participant throughout each repetition. Each trial was also visually inspected and repeated if deemed necessary by the investigator (e.g., if discontinuities were observed in the signal). After completion of the maximum voluntary contractions, 43 retroreflective markers (14 mm) were affixed to various anatomical locations on the whole body as previously described [13,16].

Each participant completed a single leg drop landing task on their right leg. Prior to performing this task, participants completed bilateral drop jump and single leg drop landing tasks in order to prepare and familiarise themselves with the experimental procedures. Participants were then required to drop off a box (height = 0.31m) and land on their right leg. The ground embedded force plate was situated immediately in front of the box. Participants were required to land with their right foot entirely within the boundaries of the force plate and, without shuffling their foot, rise from the point of peak knee flexion to standing upright (with a fully extended knee) without any other part of their body (e.g. their left foot) touching the ground at any point. Participants were informed of the criteria for a successful trial before performing the task, but no specific technique coaching was provided prior to or during testing. The first successfull trial completed by each participant was selected for subsequent analysis.

Data processing

Marker trajectories and GRFs were low-pass filtered using a zero-lag, 4th order Butterworth filter with a cut-off frequency of 15Hz. EMG data were corrected for offset, high pass filtered (20Hz), full-wave rectified and low-pass filtered (6Hz) using a zero-lag, 4th order Butterworth filter to obtain a linear envelope. EMG data were normalised to the peak amplitude (i.e.

single highest value) obtained across all trials (i.e., both the isometric maximum voluntary contractions and dynamic tasks).

Neuromusculoskeletal modelling

The neuromusculoskeletal modelling pipeline is summarised in Fig. 1. A 31 degree-of-freedom (DOF) full-body musculoskeletal model, with 80 musculotendon actuators (lower body) and 19 force/torque actuators (upper body) [18], was used to perform the musculoskeletal simulations in OpenSim [19]. Each hip was modelled as a 3-DOF ball and socket. Each knee was modelled as a 1-DOF hinge, with other rotational (valgus/varus and internal/external rotation) and translational (anteroposterior and superior-inferior) movements constrained to change as a function of the knee flexion angle [20]. Two non-intersecting pin joints were used to represent the ankle (talocrural and subtalar joints). The head-trunk segment was modelled as a single rigid segment, articulating with the pelvis via a 3-DOF ball and socket joint. Each upper limb was characterised by a 3-DOF ball and socket shoulder joint and single-DOF elbow and radioulnar joints. The generic model's segments were linearly scaled to each participant's individual anthropometry as determined during a static trial. An inverse kinematics algorithm was used to calculate joint angles by means of a least-squares optimisation that minimised the difference between model and experimental marker positions [21]. Inverse dynamics was used to obtain the joint moments acting about each modelled DOF. We then computed muscle-tendon unit lengths and moment arms about the respective joints each muscle crossed.

Muscle forces were obtained via an EMG informed approach [22,23]. We chose this approach because muscle force estimation that was entirely driven by surface EMG would have left too many muscles unaccounted for, thereby substantially limiting the scope of our analysis. Alternatively, a static optimisation algorithm for estimating muscle forces can account for these neglected muscle groups; however, our pilot analysis showed poor agreement between predicted activations and experimental EMG for certain muscle groups (e.g. hamstrings). Subsequently, the EMG informed approach incorporated the strengths of both options. To perform these simulations, the inverse dynamics derived joint moments were combined with the computed muscle-tendon lengths, muscle moment arms, and the normalised EMG signals to calibrate muscle-tendon unit parameters in the scaled musculoskeletal model [22]. This process utilised a simulated annealing algorithm to minimise the difference between experimental joint moments (from inverse dynamics) and model joint moments (product of muscle forces and their corresponding moment arms) by adjusting neuromuscular parameters (e.g., tendon slack lengths, strength coefficients) within uncertainty tolerances. After this calibration process, an EMG informed approach was used to compute muscle forces whilst adhering to the physiological force-length and force-velocity relationships of skeletal muscle [22,23]. This process involved the use of a static optimisation algorithm to decompose net joint moments into individual muscle forces by minimising the sum of activations squared, whilst also limiting the deviation of the excitation patterns from experimentally recorded EMG signals (where available). This method therefore accounted for participant-specific muscle recruitment patterns for muscles where EMG data were available and constrained the solution space for the remaining muscles.

The measured GRFs were decomposed into individual muscular contributions by using a universal “rolling on ground” constraint to model the interaction between the foot and the ground [24,25]. Each muscle’s contribution to the joint reaction forces and moments at the knee were then computed by applying each muscle’s force and contribution to the GRF in isolation and resolving the dynamical equations of motion. The computed knee joint reaction forces and moments (expressed in a tibial reference frame, Supplementary Fig. 2) represent the forces and moments that the knee joint experiences as a consequence of all motions and forces in the model, including muscles and other actuators.

Outcome variables

Outcome variables of interest were each muscle's contribution to the anteroposterior shear joint reaction force as well as the frontal and transverse plane joint reaction moments at the knee, as these variables have been shown to be associated with higher ACL loads and/or injury [7]. We restricted our analysis to the landing phase (defined as the time period from initial contact to peak knee flexion) because ACL injury typically occurs promptly after initial contact [10]. Muscular contributions were grouped according to functional groups similar to prior work [13] (see Supplementary Table 1 for full details). Note that we focused our reporting on major muscle groups, and did not report on any muscle that was not found to make a meaningful contribution to any of the three key knee joint reaction forces or moments (see Rajagopal et al. [18] for all musculotendinous actuators included in the model). Additionally, we focused our results reporting on the "typical" (i.e., mean) contributions of muscles, but due to potential clinical relevance, data describing inter-individual variability in muscle contributions are also provided in Supplementary Figs. 7-9 for the interested reader.

Validation and verification

To provide confidence in our simulations, we performed various validation and verification tests according to best practice recommendations [26]. Specifically, we confirmed that the model-based and experimental data were in agreement, where such data were available. These comparisons revealed close agreement between model and experimentally determined excitations (Supplementary Figs. 3 and 4), joint moments (Supplementary Fig. 5), and knee reaction forces and moments (Supplementary Fig. 4). Finally, we observed similar trends in the time-varying characteristics of our experimental joint angles (Supplementary Fig. 7) and inverse dynamics based joint moments (Supplementary Fig. 5) when compared with prior published data of single leg drop landing tasks from similar heights [14].

RESULTS

Anteroposterior shear joint reaction force

The net anteroposterior shear joint reaction force was characterised by an anterior shear force that peaked at 153N soon after initial contact and declined thereafter until transitioning to a posterior shear force at 14% of the landing phase (Fig. 2). The anterior shear joint reaction force was primarily produced by the quadriceps and gastrocnemius muscle groups. For these muscle groups, the peak contribution occurred within the first 20% of the landing phase, with contributions declining thereafter. The greatest peak was produced by the vasti (263N), followed by the medial gastrocnemius (249N), lateral gastrocnemius (89N) and rectus femoris (80N). Muscles that did not span the knee made relatively limited contributions to the anterior shear joint reaction force. For example, the largest non-knee-spanning contributions came from the ankle dorsi-flexors (up to 74N), gluteus maximus (up to 72N) and adductors (up to 72N). The posterior shear joint reaction force progressively increased throughout the landing phase, peaking at 744N. The greatest contributors to the posterior shear joint reaction force were the hamstrings and soleus. The contribution of the medial hamstrings and biceps femoris tended to gradually increase for the first 50% of the landing phase, peaking at 359N and 162N, respectively. The contribution from soleus to the posterior shear joint reaction force increased immediately following initial contact reaching a peak of 393N at 20% of the landing phase, before gradually declining thereafter to 241N by the end of the landing phase. At 59% of the landing phase, the vasti were found to change function and provide a small contribution to the posterior shear joint reaction force, which reached a magnitude of around 60N by the end of the landing phase.

Frontal plane joint reaction moment (varus/valgus)

A varus joint reaction moment (peak of 19Nm at 34% of landing phase) was present for the first 68% of the landing phase, whereas a valgus joint reaction moment (peak of 6Nm at the end of the landing phase) was present for the remaining portion (Fig. 3). Throughout the landing phase, non-knee-spanning muscles had the greatest capacity to oppose the valgus joint reaction moment. For example, gluteus medius was the dominant contributor to the varus joint reaction moment (ranging from 10-38Nm across the landing phase). Substantial contributions were also made by the gluteus minimus (7-22Nm) and soleus (0-20Nm). The medial hamstrings and medial gastrocnemius also contributed around 17Nm and 15Nm, respectively, to the varus joint reaction moment at the beginning of the landing phase, with both contributions declining thereafter. During the first 30% of the landing phase, the ankle plantarflexor/invertors and the biceps femoris were the primary contributors to the valgus joint reaction moment, contributing up to 21Nm and 15Nm, respectively. Whilst these contributions declined thereafter, increasing contributions to the valgus joint reaction moment were seen from the vasti (up to 26Nm) and rectus femoris (up to 7Nm).

Transverse plane joint reaction moment (internal/external rotation)

An external rotation joint reaction moment was present throughout the entire landing phase (Fig. 4). The external rotation moment was 4-7Nm for the first 10% of the landing phase. It progressively increased, peaking at 35Nm at 27% of the landing phase, then decreased to ~30Nm for the remainder of the landing phase. The dominant contributors towards this moment were the ankle plantarflexor/invertors (up to 27Nm), vasti (up to 24Nm), and rectus femoris (up to 15Nm). An internal rotation joint reaction moment was generated by the soleus (up to 20Nm) followed by the medial hamstrings (up to 7Nm), gluteus maximus (up to 5Nm) and lateral gastrocnemius (up to 5Nm).

DISCUSSION

This study has revealed that both knee-spanning and non-knee-spanning muscles contribute to the knee joint reaction forces and moments during a single leg drop landing task. Notably, we found the hamstrings and the soleus muscles to have the greatest potential to oppose the anterior shear joint reaction force, whilst the non-knee-spanning gluteus medius, gluteus minimus and soleus muscles had the greatest potential to oppose the valgus joint reaction moment. To the authors' knowledge, no previous studies have calculated the contributions of both knee-spanning and non-knee-spanning muscles to these critical mechanical loads at the knee during a single leg drop landing task.

Anteroposterior shear joint reaction force

The anterior shear force at the knee has consistently been associated with ACL loading [7,8,27]. Studies that have investigated how muscles contribute to anteroposterior shear forces have typically focused on the quadriceps and hamstring muscle groups [11]. Findings from the current study (Figs. 2A and C) are consistent with prior research regarding the importance of these two muscles for modulating anteroposterior shear forces. Furthermore, our findings revealed that other muscles (including those that do not span the knee) also have the potential to modulate anteroposterior shear forces. For example, we found that during a single leg drop landing task, the soleus provided the largest contribution to the posterior shear joint reaction force of any single muscle (Fig. 2D). This result is consistent with our previous observations for unanticipated sidestep cutting [13] and what has been previously reported by Mokhtarzadeh and colleagues [14] for a single leg drop landing task (albeit using an alternative modelling approach). In contrast to the function of soleus, it seems that the biarticular gastrocnemius is an ACL antagonist during a single leg drop landing task, a finding that we observed (Fig. 2B) along with Mokhtarzadeh et al. [14]. Such a conclusion is substantiated by in-vivo work showing that electrical stimulation of the gastrocnemius resulted in increased ACL strain [28]. Thus, it would appear that the primary ankle plantar flexors have a similar role to the quadriceps and hamstrings with regards to the modulation of anteroposterior shear forces.

With the exception of the soleus, our data suggests that non-knee-spanning muscles made relatively small contributions to anteroposterior shear forces compared to knee-spanning muscles like the quadriceps, hamstrings and gastrocnemius (Fig. 2). However, this result is not entirely consistent with prior literature. For example, a previous study [29] investigating a lunge movement suggested that the gluteus maximus can induce a posterior shear force at the knee, whilst our data suggests that the gluteus maximus mainly contributes to an anterior shear force (Fig. 2E). This discrepancy is most likely explained by the fact that our study did not model the iliotibial band. As a consequence of this simplification, our analysis did not account for direct transmission of gluteus maximus force to the tibia via its attachment to the iliotibial band. Whilst the exclusion of the iliotibial band from our model was unlikely to have influenced the majority of our results, the role of the gluteus maximus may need to be interpreted with the aforementioned limitation kept in mind.

Frontal and transverse plane joint reaction moments

Like prior work in sidestep cutting [13] and walking [30], this study has demonstrated that the gluteus medius has the greatest capacity to oppose the valgus joint reaction moment at the knee during a single leg drop landing task. Other muscles also contributed to the frontal plane joint reaction moment at the knee (e.g. hamstrings, soleus, ankle plantarflexor/invertors) and rather interestingly there seemed to be a temporal variation in the primary muscular strategy modulating this moment. Immediately following initial contact, the frontal plane joint reaction moment was primarily modulated by opposing contributions from the medial and lateral hamstrings. These contributions rapidly declined by 25% of the landing phase, coinciding with increased contributions from the soleus and the ankle plantarflexor/invertors producing varus and valgus moments, respectively. These contributions peaked at ~25% of the landing phase. During the second half of the landing phase, the gluteus medius and minimus began providing the largest contributions to the varus joint reaction moment, whereas the quadriceps provided the largest contribution to the valgus joint reaction moment at this time. This time-dependent variation in the modulation of frontal plane knee joint loading is, to our knowledge, previously unreported.

We note that the functional role of the majority of the aforementioned muscles are generally consistent with prior work for sidestep cutting and walking [13,30]; however, there is some inconsistency in the reported role of soleus with respect to the frontal plane joint reaction moment at the knee. This inconsistency in the reported function of the soleus could be due to task-based differences between our work and prior work. It could also be attributable to the foot-ground contact model because prior research has shown predictions of muscle function for certain muscles to be sensitive to the particular foot-ground contact model [25]. Specifically, estimates of how the soleus contributes to the mediolateral GRF can be opposing when comparing the “rolling on ground” constraint used in the present work versus the multipoint constraint used in our previous work [13] and that of Sritharan and colleagues [30]. The multipoint constraint was not implemented in the present study as our pilot analysis showed poor performance (e.g. large superposition errors) in our single leg drop landing trials. This outcome may have been because the multipoint constraint set was specifically developed to estimate muscle function during relatively planar locomotion tasks such as walking and running [31]. The “rolling on ground” constraint was justified for the present study since it adequately described movement of the foot relative to the ground in the chosen task, showed low superposition errors, and has been applied in prior published work [24,32]. Nevertheless, based on the apparent sensitivity of the predicted function for soleus to the chosen foot-ground model, we recommend keeping this point in mind when interpreting results regarding the contribution of soleus to the frontal and transverse plane joint reaction moments.

Clinical implications

Prior work suggests that ACL loads are greatest when the knee joint is exposed to an anterior shear force together with a valgus and an internal rotation moment [7,8]. This specific loading combination was not observed to occur simultaneously in our data (Figs. 3-5); however, identifying the function of a specific muscle still requires consideration of its mechanical effect across multiple planes.

Based on the findings from this study, we suggest that injury prevention strategies should focus on optimising the function of the hamstrings and soleus as well as gluteus medius and minimus. Collectively, the hamstrings and soleus were found to be the dominant contributors to the posterior shear joint reaction force during the single leg drop landing task. The relative importance of non-sagittal knee joint moments with respect to ACL loading is not universally accepted [33], whereas anterior and posterior shear forces have been consistently shown to load and unload the ACL, respectively [7,8,27]. Since ACL injury occurs promptly after initial contact [10], the soleus may be particularly important for reducing the likelihood of ACL injury, as it makes a more substantial contribution to the posterior shear joint reaction force during the first 25% of the landing phase. However, although our findings suggest that the hamstrings are less effective at producing a posterior shear joint reaction force during the early stage of the landing phase, they do appear to be effective at modulating both frontal (Fig. 3C) and transverse plane (Fig. 4C) joint reaction moments following initial contact. Additionally, from a practical perspective, the function of the soleus may be difficult to isolate from the gastrocnemius (a muscle which we found to be a primary contributor to the anterior shear joint reaction force at the knee).

The gluteus medius and minimus muscles were the dominant contributors to the varus joint reaction moment, and thus probably have best potential to modulate the magnitude of the valgus joint reaction moment (Fig. 3E). Importantly, this finding holds true across studies that have used different modelling techniques and have investigated different tasks [13,30]. When these results are interpreted together with results from prospective studies showing that higher knee valgus loading [34] and lower hip abduction strength [35] are associated with ACL injury, it appears that the gluteus medius and minimus may be especially important muscles to consider in injury prevention programs.

Limitations

Whilst our study has revealed some novel insights, we acknowledge that there are some limitations to this work. One limitation is that the present study only involved a cohort of eight healthy recreationally active males performing a laboratory-controlled drop-landing task. It is unclear if our findings would hold true if the demands of sport-specific injurious scenarios were more closely replicated (e.g., unplanned landings). For example, whilst the net joint reaction forces and moments in this study compare well to previous work employing similar methodology (e.g., [13]), the net frontal and transverse moments observed were substantially less than the >200Nm moments directly measured during in-vitro simulation of ACL rupture [36]. In such “high risk” scenarios, it is possible that muscle induced reaction forces and moments may have limited capacity to protect the ACL from rupture. Practical and ethical constraints make studying “high risk” scenarios very difficult under in-vivo conditions, thus future research might aim to develop techniques (e.g., in-vitro or in-silico) to investigate muscle induced reaction forces and moments under these scenarios. Additionally, such research should also consider the influence of different populations such as females, specific athletic subgroups, and pathological populations.

Another limitation is that we did not compute ACL forces directly. Whilst including knee ligaments into the musculoskeletal model would have allowed us to predict ligament (or ACL) forces directly, this complexity would come at the cost of introducing additional uncertainties related to in-vivo ligament properties [37]. Due to the sensitivity of estimated ACL forces to these ligament properties (e.g., reference strains and ligament stiffness) [37], we opted to exclude ligaments from the model. Nevertheless, based on the findings from previous studies [7,8,38], we are confident that the primary outcome measures used in the present represent appropriate surrogate indicators of ACL loading.

The decision to exclude ligaments from the model meant that translations and non-sagittal rotations at the knee needed to be constrained as a function of the knee flexion angle [20], similar to prior studies [14], in order to ensure our predicted muscle forces were as valid as possible. Another advantage of adopting such constraints is minimising the impact of soft tissue artefact. Prior research has shown that non-sagittal plane knee rotations are particularly sensitive to soft tissue artefact when using skin-mounted marker systems [39], especially for high-impact tasks. Whilst soft tissue artefact can influence all joint angles, we used a global optimisation inverse kinematics algorithm to obtain our joint angles, which has previously been shown to be capable of minimising the influence of soft tissue artefact [21].

Muscle forces estimated in the present work cannot be directly validated, as in-vivo muscle forces are not practically feasible to measure [40]. However, the EMG informed approach utilised has been shown to be capable of yielding reasonable predictions of in-vivo joint contact forces [41], which serves as an indirect validation of muscle forces due to the high dependency of joint contact forces on muscle forces [40]. Furthermore, the EMG informed approach was found to be successful in its aim of generating a set of muscle excitations that matched experimentally recorded EMG signals (whilst also producing joint moments that matched inverse-dynamics derived joint moments), and thus helped to ensure that time-varying trends in our predicted muscle forces were physiologically plausible and participant specific (see Supplementary Figs. 7-9 for participant-specific data). Where EMG data were not collected for certain muscles in the present study, but reported by other studies investigating similar tasks, we found favourable comparisons to the predicted excitation patterns in our work (Supplementary Fig. 4). Nevertheless, we acknowledge that EMG data were not available for all muscles, hence the excitations for all investigated muscle groups could not be validated.

Conclusion

In conclusion, this study demonstrated that knee-spanning as well as non-knee-spanning muscles contribute substantially to anteroposterior shear joint reaction forces as well as frontal and transverse plane joint reaction moments at the knee during a single leg drop landing task. Specifically, the quadriceps and gastrocnemius muscles were found to be the major contributors to the anterior shear joint reaction force, whilst the hamstrings and the soleus were the major contributors to the posterior shear joint reaction force. The valgus joint reaction moment was primarily produced by both knee-spanning (vasti) and non-knee-spanning (ankle plantarflexor/invertors) muscles. This moment was opposed by the non-knee-spanning gluteus medius, gluteus minimus and soleus. The external rotation joint reaction moment throughout the landing phase was primarily generated by the ankle plantarflexor/invertors and the vasti. Based on our consideration of multiple loading states, we conclude that the hamstrings (biceps femoris and medial hamstrings), soleus, as well as gluteus medius and minimus to have the greatest potential to offset ACL loading during a single leg drop landing task. Optimising the function of these muscles should therefore be of high priority in injury prevention programs.

PERSPECTIVE

Based on prior work (e.g. [11,28]), researchers and clinicians may be tempted to focus on knee-spanning muscles in order to modulate knee joint forces in ACL injury prevention programs. However, this study shows that non-knee-spanning muscles play a substantial role in modulating knee joint reaction forces and moments during a single leg drop landing task. For example, the gluteus medius induced knee varus loading (thus opposing knee valgus loading) of up to 38Nm, which is more than 2-fold higher than any knee-spanning muscle. Similarly, the non-knee-spanning soleus induced a posterior shear force of a substantial magnitude (up to 393N), which exceeded that from either the medial or lateral hamstrings. The findings from the present study can therefore be used to inform interventions aiming to reduce ACL injury risk.

References

1. Joseph AM, Collins CL, Henke NM, Yard EE, Fields SK, Comstock RD. A multisport epidemiologic comparison of anterior cruciate ligament injuries in high school athletics. *Journal of athletic training.* 2013;48(6):810-817.
2. Ardern CL, Webster KE, Taylor NF, Feller JA. Return to the preinjury level of competitive sport after anterior cruciate ligament reconstruction surgery: two-thirds of patients have not returned by 12 months after surgery. *The American journal of sports medicine.* 2011;39(3):538-543.
3. Janssen KW, Orchard JW, Driscoll TR, van Mechelen W. High incidence and costs for anterior cruciate ligament reconstructions performed in Australia from 2003-2004 to 2007-2008: time for an anterior cruciate ligament register by Scandinavian model? *Scandinavian journal of medicine & science in sports.* 2012;22(4):495-501.
4. Wiggins AJ, Grandhi RK, Schneider DK, Stanfield D, Webster KE, Myer GD. Risk of Secondary Injury in Younger Athletes After Anterior Cruciate Ligament Reconstruction: A Systematic Review and Meta-analysis. *The American journal of sports medicine.* 2016;44(7):1861-1876.
5. Øiestad BE, Engebretsen L, Storheim K, Risberg MA. Knee Osteoarthritis After Anterior Cruciate Ligament Injury: A Systematic Review. *The American journal of sports medicine.* 2009;37(7):1434-1443.
6. Wojtys EM, Beaulieu ML, Ashton-Miller JA. New perspectives on ACL injury: On the role of repetitive sub-maximal knee loading in causing ACL fatigue failure. *Journal of orthopaedic research : official publication of the Orthopaedic Research Society.* 2016;34(12):2059-2068.
7. Markolf KL, Burchfield DM, Shapiro MM, Shepard MF, Finerman GA, Slauterbeck JL. Combined knee loading states that generate high anterior cruciate ligament forces. *Journal of orthopaedic research : official publication of the Orthopaedic Research Society.* 1995;13(6):930-935.
8. Kiapour AM, Demetropoulos CK, Kiapour A, et al. Strain Response of the Anterior Cruciate Ligament to Uniplanar and Multiplanar Loads During Simulated Landings: Implications for Injury Mechanism. *The American journal of sports medicine.* 2016;44(8):2087-2096.
9. Koga H, Nakamae A, Shima Y, et al. Mechanisms for Noncontact Anterior Cruciate Ligament Injuries: Knee Joint Kinematics in 10 Injury Situations From Female Team

Handball and Basketball. *The American journal of sports medicine.* 2010;38(11):2218-2225.

10. Krosshaug T, Nakamae A, Boden BP, et al. Mechanisms of Anterior Cruciate Ligament Injury in Basketball: Video Analysis of 39 Cases. *The American journal of sports medicine.* 2007;35(3):359-367.
11. Biscarini A, Benvenuti P, Botti FM, Brunetti A, Brunetti O, Pettorossi VE. Voluntary enhanced cocontraction of hamstring muscles during open kinetic chain leg extension exercise: its potential unloading effect on the anterior cruciate ligament. *The American journal of sports medicine.* 2014;42(9):2103-2112.
12. Zajac FE, Gordon ME. Determining muscle's force and action in multi-articular movement. *Exerc Sport Sci Rev.* 1989;17(1):187-230.
13. Maniar N, Schache AG, Sritharan P, Opar DA. Non-knee-spanning muscles contribute to tibiofemoral shear as well as valgus and rotational joint reaction moments during unanticipated sidestep cutting. *Sci Rep.* 2018;8(1):2501.
14. Mokhtarzadeh H, Yeow CH, Hong Goh JC, Oetomo D, Malekipour F, Lee PV-S. Contributions of the Soleus and Gastrocnemius muscles to the anterior cruciate ligament loading during single-leg landing. *J Biomech.* 2013;46(11):1913-1920.
15. Maniar N, Bryant AL, Sritharan P, Schache AG, Opar DA. Muscle contributions to medial and lateral tibiofemoral compressive loads during sidestep cutting. *Journal of biomechanics.* 2020;101:109641.
16. Maniar N, Schache AG, Cole MH, Opar DA. Lower-limb muscle function during sidestep cutting. *Journal of biomechanics.* 2019;82:186-192.
17. Hermens HJ, Freriks B, Disselhorst-Klug C, Rau G. Development of recommendations for SEMG sensors and sensor placement procedures. *Journal of electromyography and kinesiology : official journal of the International Society of Electrophysiological Kinesiology.* 2000;10(5):361-374.
18. Rajagopal A, Dembia CL, DeMers MS, Delp DD, Hicks JL, Delp SL. Full-Body Musculoskeletal Model for Muscle-Driven Simulation of Human Gait. *IEEE transactions on bio-medical engineering.* 2016;63(10):2068-2079.
19. Delp SL, Anderson FC, Arnold AS, et al. OpenSim: open-source software to create and analyze dynamic simulations of movement. *IEEE transactions on bio-medical engineering.* 2007;54(11):1940-1950.
20. Walker PS, Rovick JS, Robertson DD. The effects of knee brace hinge design and placement on joint mechanics. *Journal of biomechanics.* 1988;21(11):965-974.

21. Lu T-W, O'connor J. Bone position estimation from skin marker co-ordinates using global optimisation with joint constraints. *J Biomech.* 1999;32(2):129-134.
22. Pizzolato C, Lloyd DG, Sartori M, et al. CEINMS: A toolbox to investigate the influence of different neural control solutions on the prediction of muscle excitation and joint moments during dynamic motor tasks. *J Biomech.* 2015;48(14):3929-3936.
23. Sartori M, Farina D, Lloyd DG. Hybrid neuromusculoskeletal modeling to best track joint moments using a balance between muscle excitations derived from electromyograms and optimization. *J Biomech.* 2014;47(15):3613-3621.
24. Hamner SR, Delp SL. Muscle contributions to fore-aft and vertical body mass center accelerations over a range of running speeds. *J Biomech.* 2013;46(4):780-787.
25. Dorn TW, Lin Y-C, Pandy MG. Estimates of muscle function in human gait depend on how foot-ground contact is modelled. *Comput Methods Biomech Biomed Engin.* 2012;15(6):657-668.
26. Hicks JL, Uchida TK, Seth A, Rajagopal A, Delp SL. Is My Model Good Enough? Best Practices for Verification and Validation of Musculoskeletal Models and Simulations of Movement. *J Biomech Eng.* 2015;137(2):020905.
27. Fleming BC, Renstrom PA, Beynnon BD, et al. The effect of weightbearing and external loading on anterior cruciate ligament strain. *J Biomech.* 2001;34(2):163-170.
28. Fleming BC, Renstrom PA, Ohlen G, et al. The gastrocnemius muscle is an antagonist of the anterior cruciate ligament. *Journal of orthopaedic research : official publication of the Orthopaedic Research Society.* 2001;19(6):1178-1184.
29. Alkjaer T, Wieland MR, Andersen MS, Simonsen EB, Rasmussen J. Computational modeling of a forward lunge: towards a better understanding of the function of the cruciate ligaments. *J Anat.* 2012;221(6):590-597.
30. Sritharan P, Lin YC, Pandy MG. Muscles that do not cross the knee contribute to the knee adduction moment and tibiofemoral compartment loading during gait. *Journal of orthopaedic research : official publication of the Orthopaedic Research Society.* 2012;30(10):1586-1595.
31. Lin YC, Kim HJ, Pandy MG. A computationally efficient method for assessing muscle function during human locomotion. *Int J Numer Method Biomed Eng.* 2011;27(3):436-449.
32. Dixon PC, Jansen K, Jonkers I, Stebbins J, Theologis T, Zavatsky AB. Muscle contributions to centre of mass acceleration during turning gait in typically developing children: A simulation study. *J Biomech.* 2015;48(16):4238-4245.

33. Hashemi J, Breighner R, Chandrashekar N, et al. Hip extension, knee flexion paradox: a new mechanism for non-contact ACL injury. *J Biomech.* 2011;44(4):577-585.
34. Hewett TE, Myer GD, Ford KR, et al. Biomechanical measures of neuromuscular control and valgus loading of the knee predict anterior cruciate ligament injury risk in female athletes: a prospective study. *The American journal of sports medicine.* 2005;33(4):492-501.
35. Khayambashi K, Ghoddosi N, Straub RK, Powers CM. Hip muscle strength predicts noncontact anterior cruciate ligament injury in male and female athletes: a prospective study. *The American journal of sports medicine.* 2016;44(2):355-361.
36. Ueno R, Navacchia A, Bates NA, Schilaty ND, Krych AJ, Hewett TE. Analysis of Internal Knee Forces Allows for the Prediction of Rupture Events in a Clinically Relevant Model of Anterior Cruciate Ligament Injuries. *Orthop J Sports Med.* 2020;8(1):2325967119893758.
37. Smith CR, Vignos MF, Lenhart RL, Kaiser J, Thelen DG. The Influence of Component Alignment and Ligament Properties on Tibiofemoral Contact Forces in Total Knee Replacement. *J Biomech Eng.* 2016;138(2):021017.
38. Oh YK, Lipps DB, Ashton-Miller JA, Wojtys EM. What strains the anterior cruciate ligament during a pivot landing? *The American journal of sports medicine.* 2012;40(3):574-583.
39. Benoit DL, Ramsey DK, Lamontagne M, Xu L, Wretenberg P, Renström P. Effect of skin movement artifact on knee kinematics during gait and cutting motions measured in vivo. *Gait Posture.* 2006;24(2):152-164.
40. Pandy MG, Andriacchi TP. Muscle and joint function in human locomotion. *Annu Rev Biomed Eng.* 2010;12:401-433.
41. Hoang HX, Pizzolato C, Diamond LE, Lloyd DG. Subject-specific calibration of neuromuscular parameters enables neuromusculoskeletal models to estimate physiologically plausible hip joint contact forces in healthy adults. *J Biomech.* 2018;80:111-120.

Figure legends

Figure 1. Musculoskeletal modelling pipeline used to generate simulations of single leg drop landing task from a 0.31m height. The top panel identifies the experimental data, which include three-dimensional marker trajectories, three-dimensional ground reaction forces (GRF), and surface electromyography (EMG). The bottom panel illustrates the flow of modelling steps and their outputs. Note that the EMG-assisted optimisation step also involves a calibration of neuromusculoskeletal parameters, described in full detail elsewhere [22]. Note that induced GRFs are much smaller in magnitude than induced joint loads, and are subsequently not illustrated on the same scale for perceptibility reasons.

Figure 2. Mean contributions of muscles to knee anteroposterior shear joint reaction force for the landing phase (initial contact to peak knee flexion) of a single leg drop landing task from a 0.31m height. Positive values indicate anterior shear force. Note that the shaded grey represents the experimental value (net value accounting for all forces) for each reaction load. RECFEM, rectus femoris; VASTI, vasti (vastus intermedius, lateralis and medialis); GASLAT, gastrocnemius lateralis; GASMED, gastrocnemius medialis; BFEM, biceps femoris (biceps femoris long head and short head), SEMI, medial hamstrings (semitendinosus and semimembranosus); SOLEUS, soleus; PFINV, plantar-flexor-invertors (tibialis posterior, flexor digitorum longus and flexor hallucis longus); PER, peroneus (peroneus brevis and longus); GMAX, gluteus maximus; GMED, gluteus medius; GMIN, gluteus minimus; ILPSO, iliopsoas (iliacus and psoas major); ADD, adductors (adductor brevis, longus and magnus); DORSI, dorsiflexors (tibialis anterior, extensor digitorum and hallucis longus).

Figure 3. Mean contributions of muscles to knee valgus/varus reaction moment for the landing phase (initial contact to peak knee flexion) of a single leg drop landing task from a 0.31m height. Positive values indicate varus moment. Note that the shaded grey represents

the experimental value (net value accounting for all forces) for each reaction load. RECFEM, rectus femoris; VASTI, vasti (vastus intermedius, lateralis and medialis); GASLAT, gastrocnemius lateralis; GASMED, gastrocnemius medialis; BFEM, biceps femoris (biceps femoris long head and short head), SEMI, medial hamstrings (semitendinosus and semimembranosus); SOLEUS, soleus; PFINV, plantar-flexor-invertors (tibialis posterior, flexor digitorum longus and flexor hallucis longus); PER, peroneus (peroneus brevis and longus); GMAX, gluteus maximus; GMED, gluteus medius; GMIN, gluteus minimus; ILPSO, iliopsoas (iliacus and psoas major); ADD, adductors (adductor brevis, longus and magnus); DORSI, dorsiflexors (tibialis anterior, extensor digitorum and hallucis longus).

Figure 4. Mean contributions of muscles to knee internal/external rotation reaction moment for the landing phase (initial contact to peak knee flexion) of a single leg drop landing task from a 0.31m height. Positive values indicate internal rotation moment. Note that the shaded grey represents the experimental value (net value accounting for all forces) for each reaction load. RECFEM, rectus femoris; VASTI, vasti (vastus intermedius, lateralis and medialis); GASLAT, gastrocnemius lateralis; GASMED, gastrocnemius medialis; BFEM, biceps femoris (biceps femoris long head and short head), SEMI, medial hamstrings (semitendinosus and semimembranosus); SOLEUS, soleus; PFINV, plantar-flexor-invertors (tibialis posterior, flexor digitorum longus and flexor hallucis longus); PER, peroneus (peroneus brevis and longus); GMAX, gluteus maximus; GMED, gluteus medius; GMIN, gluteus minimus; ILPSO, iliopsoas (iliacus and psoas major); ADD, adductors (adductor brevis, longus and magnus); DORSI, dorsiflexors (tibialis anterior, extensor digitorum and hallucis longus).

Contributorship

Conception of experimental procedures – NM, AGS & DAO. Conception of data analysis – NM. Data collection and analysis – NM. Preparation of Figures – NM. Interpretation of data – NM, AGS, CP, & DAO. Writing of manuscript – NM, AGS, CP & DAO.

Conflict of interest statement

Authors have no conflicts of interest to declare.

Funding

NM was supported by the Australian Government Research Training Program Scholarship.

Appendices

The following pages contain supplementary information for the manuscript: “Lower-limb muscle force contributions to tibiofemoral shear forces and valgus and rotational joint moments during single leg landing”. The material includes four figures demonstrating the definition of the tibial reference frame, a comparison of the experimental and model excitations, a comparison of experimental and model joint moments, a comparison of reaction forces derived from model and experimental ground reaction forces, and the experimental joint angles. A supplementary table also identifies all the actuators used in the model, their functional grouping, and excitation inputs. A separate reference list for the Appendices is also provided.

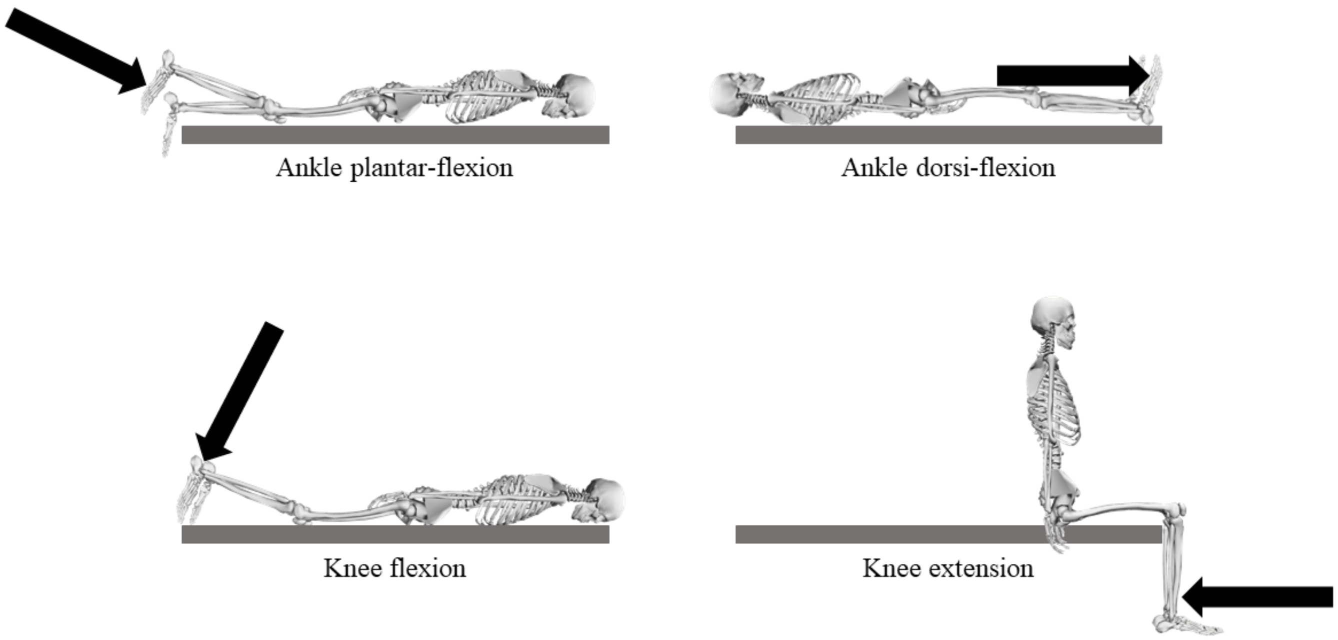

Supplementary Figure 1. Participant positions during isometric maximum voluntary contractions for the purposes of electromyography (EMG) normalisation. The black arrow indicates the direction of resistance applied. Note that for ankle plantar-flexion, the resistance was provided by a rigid wall, with the investigator providing support against the shoulders of the participant. For all other tests, firm resistance was provided directly by the investigator at the location indicated by the black arrow. All contractions were held for at least 3 seconds, whilst the investigator provided strong verbal encouragement throughout.

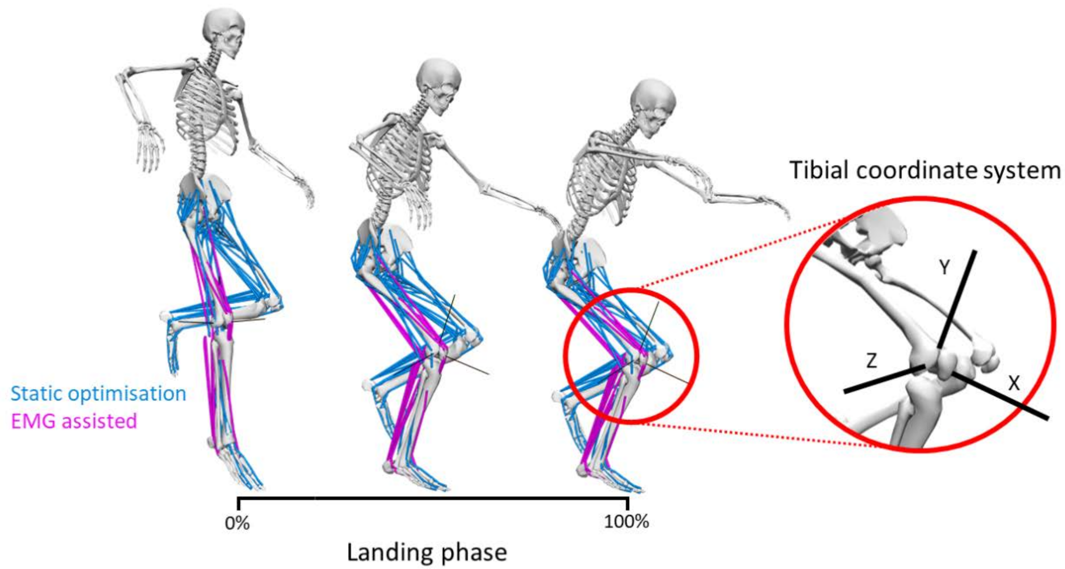

Supplementary Figure 2. Visualisation of the landing phase (initial contact to peak knee flexion) for a single leg drop landing task from a 0.31m height. Musculotendon actuator are coloured according to the method of muscle force estimation, either via static optimisation or electromyography (EMG) assisted optimisation. The final panel also identifies the tibial reference frame used to describe the joint reaction forces and moments in the main article. The tibial reference frame was defined as follows: Y, superior-inferior axis; X, anteroposterior axis; Z, mediolateral axis. The anteroposterior shear force was expressed along the X (anteroposterior) axis, whilst the valgus and rotational moments were expressed about the X (anteroposterior) and Y (superior-inferior) axes, respectively.

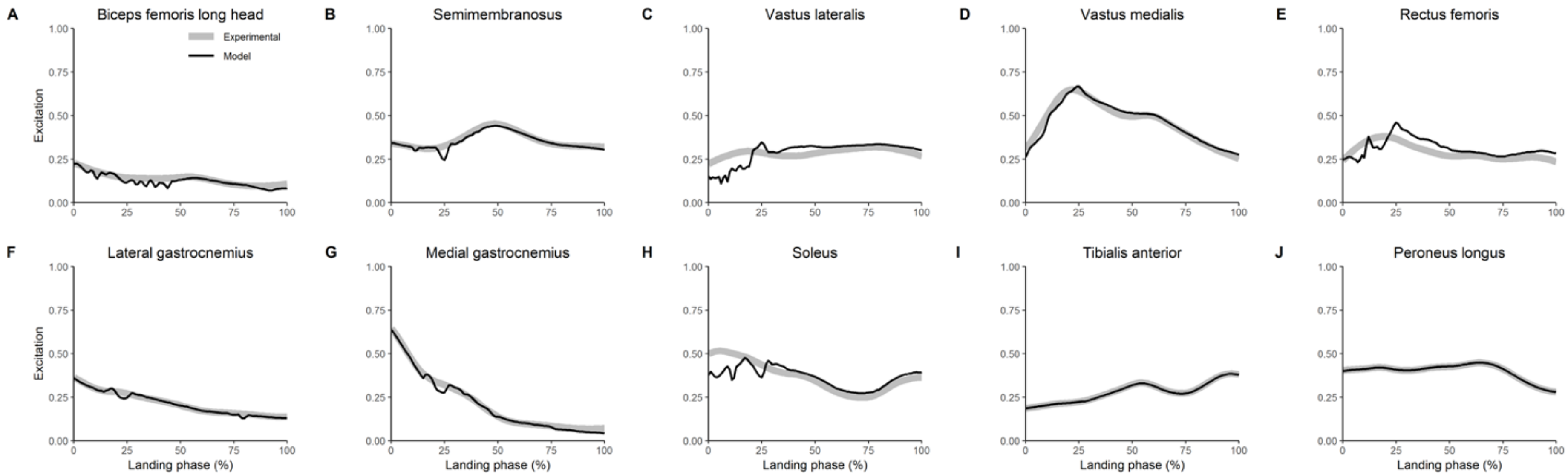

Supplementary Figure 3. Comparison of the mean model (black) and experimental (grey, from surface electromyography) excitations from 8 participants for the landing phase (initial contact to peak knee flexion) of a single leg drop landing task from a 0.31m height.

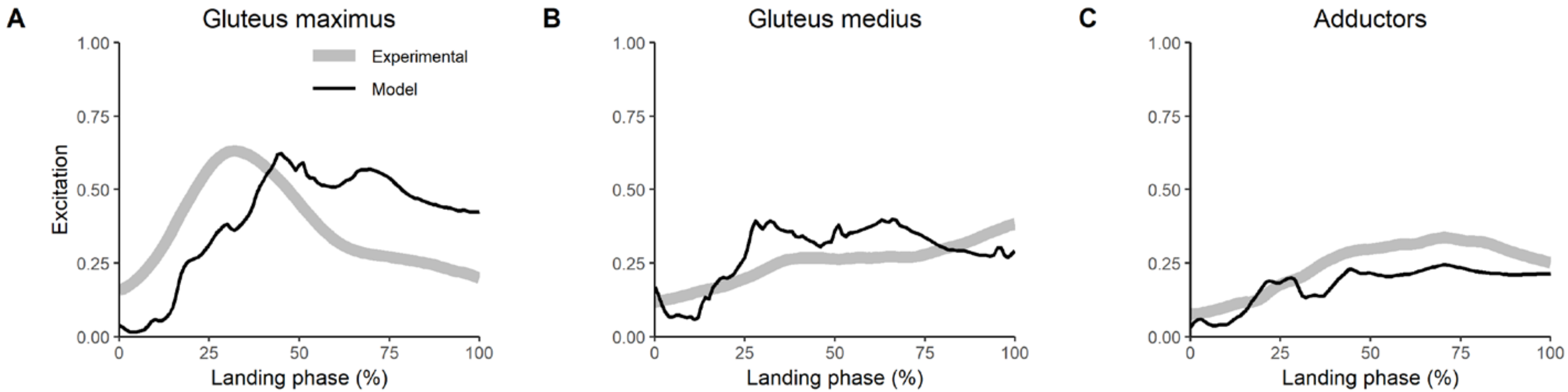

Supplementary Figure 4. Comparison of the mean model (black) and experimental (grey, from surface electromyography) excitations. Model excitations were generated from 8 participants for the landing phase (initial contact to peak knee flexion) of a single leg drop landing task from a 0.31m height. Experimental data for each panel obtained from the literature as follows: A, landing phase of single leg drop landing from 0.50m height [1]; B, landing phase of bilateral drop jump from 0.31m height [2]; C, landing phase of bilateral drop jump from 0.31m height [2].

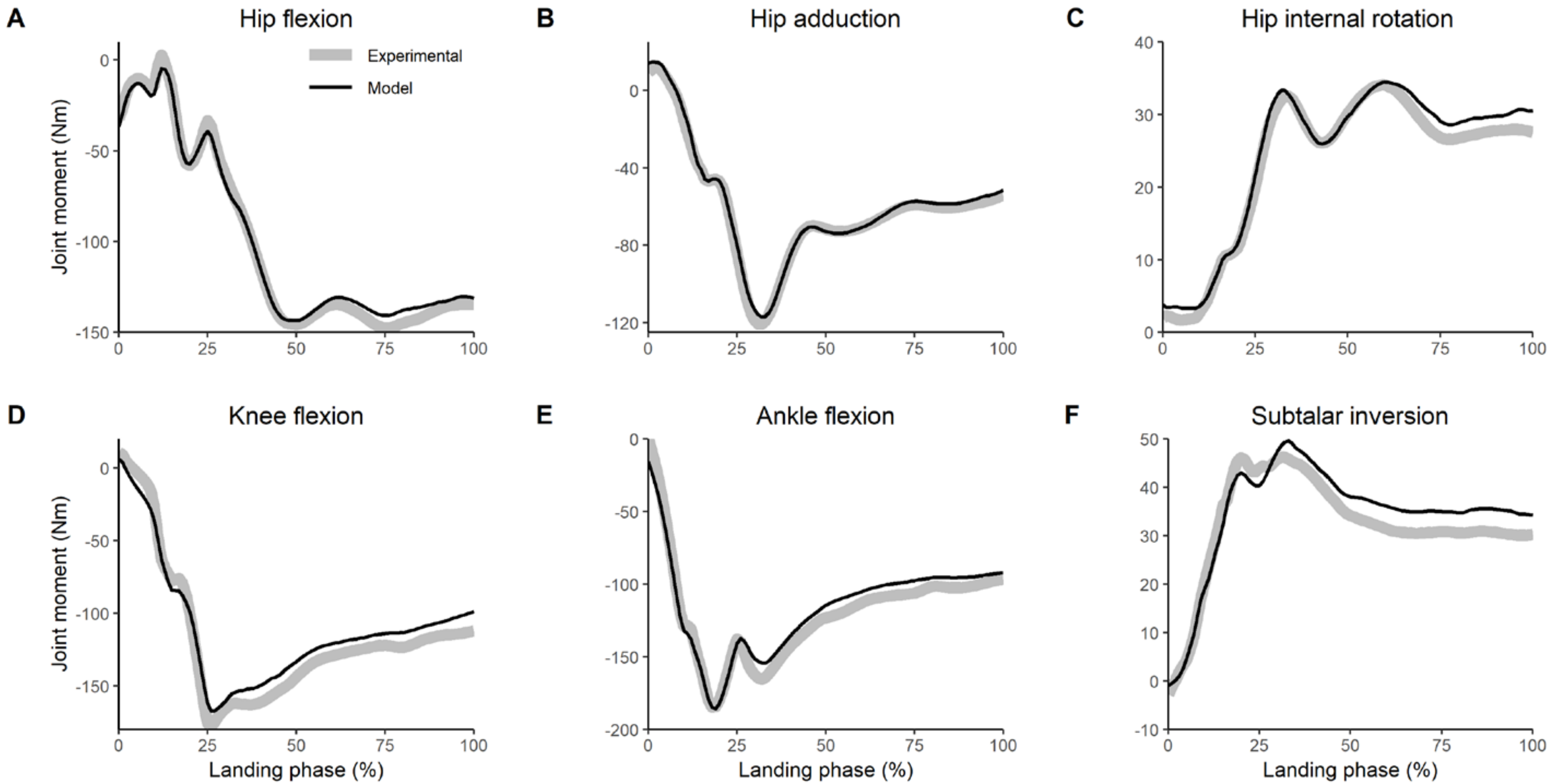

Supplementary Figure 5. Comparison of the mean model (black) and experimental (grey, from inverse dynamics) joint moments from 8 participants for the landing phase (initial contact to peak knee flexion) of a single leg drop landing task from a 0.31m height. Positive values are indicated by the title of each subplot.

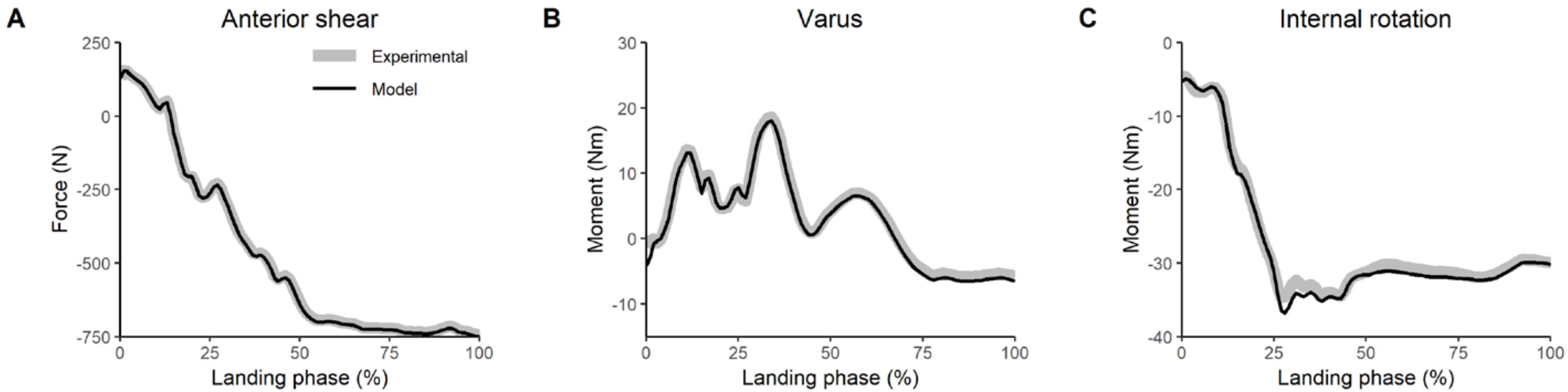

Supplementary Figure 6. Comparison of the mean joint reaction shear forces (A), varus moments (B) and rotation moments (C) derived from model (black) and experimental (grey) ground reaction forces from 8 participants for the landing phase (initial contact to peak knee flexion) of a single leg drop landing task from a 0.31m height. Positive values are indicated by the title of each subplot.

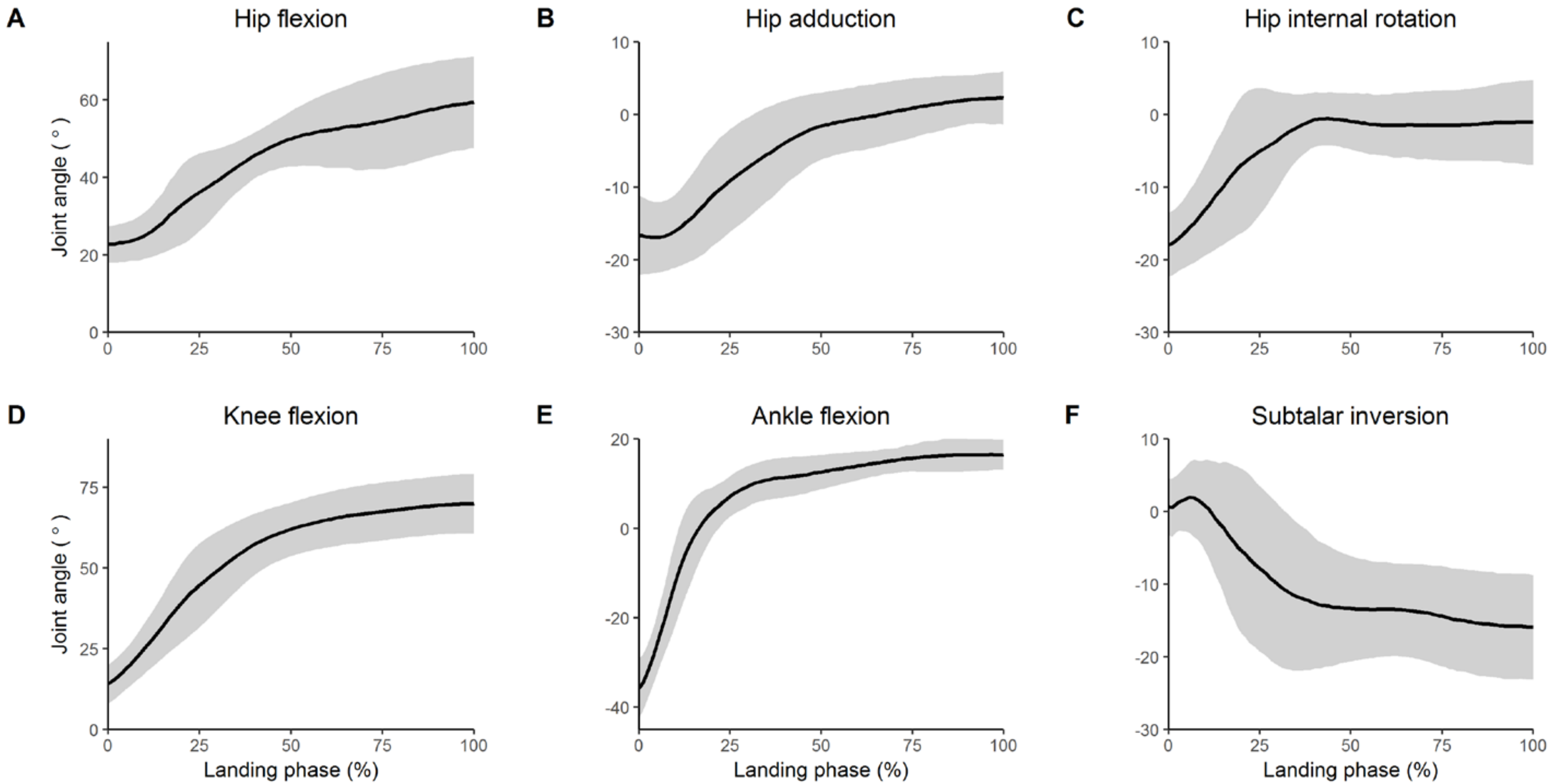

Supplementary Figure 7. Mean (black line) and SD (grey shaded) lower-limb joint angles from 8 participants for the landing phase (initial contact to peak knee flexion) of a single leg drop landing task from a 0.31m height. Positive values are indicated by the title of each subplot.

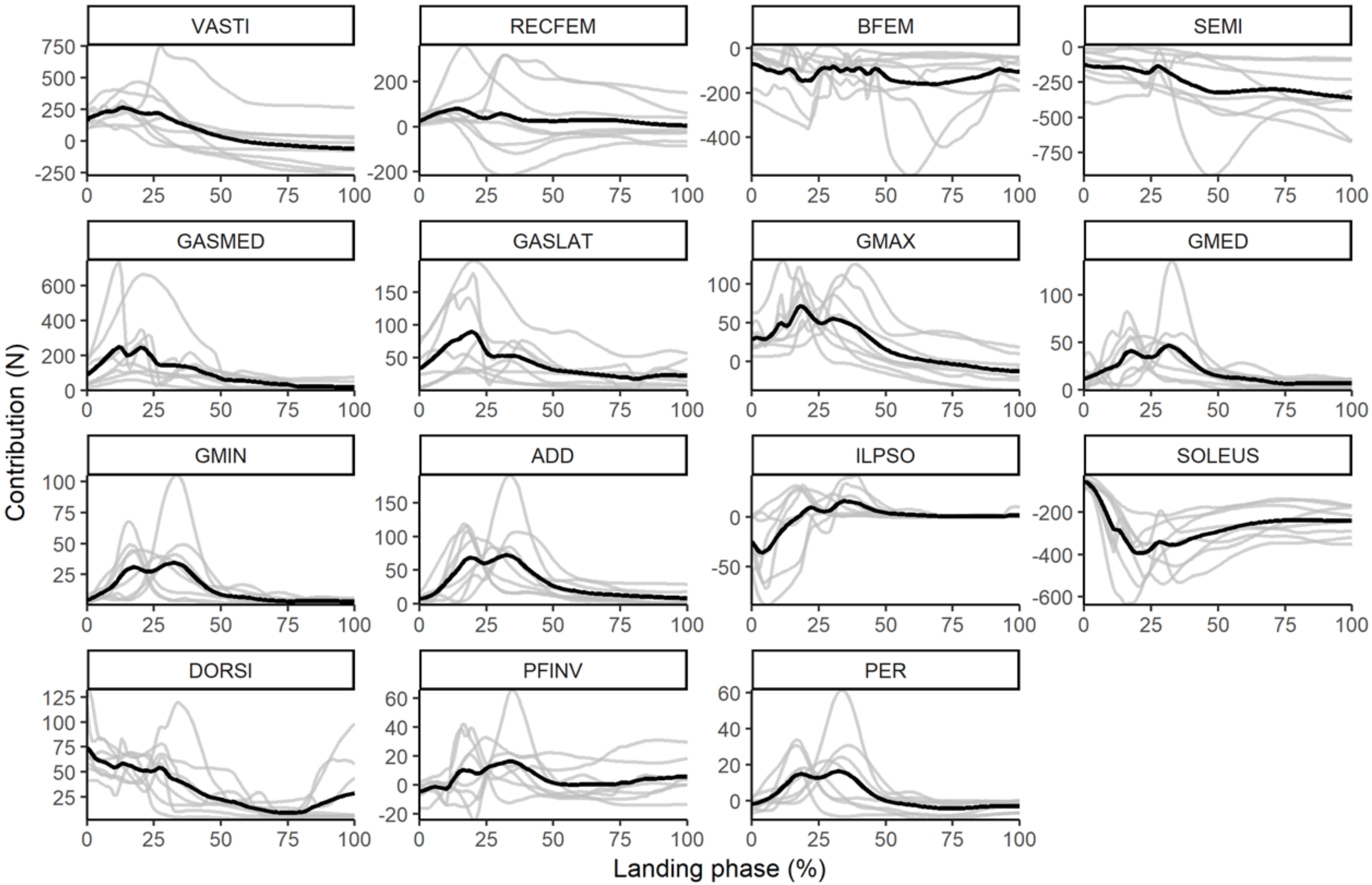
VASTI
RECFEM
BFEM
SEMI
GASMED
GASLAT
GMAX
GMED
GMIN
ADD
ILPSO
SOLEUS
DORSI
PFINV
PER
Contribution (N)
Landing phase (%)

Supplementary Figure 7. Mean (black line) and individual participant (grey line) contributions of muscles to knee anterioroposterior shear reaction force for the landing phase (initial contact to peak knee flexion) of a single leg drop landing task from a 0.31m height. Positive values indicate anterior shear force. RECFEM, rectus femoris; VASTI, vasti (vastus intermedius, lateralis and medialis); GASLAT, gastrocnemius lateralis; GASMED, gastrocnemius medialis; BFEM, biceps femoris (biceps femoris long head and short head), SEMI, medial hamstrings (semitendinosus and semimembranosus); SOLEUS, soleus; PFINV, plantar-flexor-invertors (tibialis posterior, flexor digitorum longus and flexor hallucis longus); PER, peroneus (peroneus brevis and longus); GMAX, gluteus maximus; GMED, gluteus medius; GMIN, gluteus minimus; ILPSO, iliopsoas (iliacus and psoas major); ADD, adductors (adductor brevis, longus and magnus); DORSI, dorsiflexors (tibialis anterior, extensor digitorum and hallucis longus).

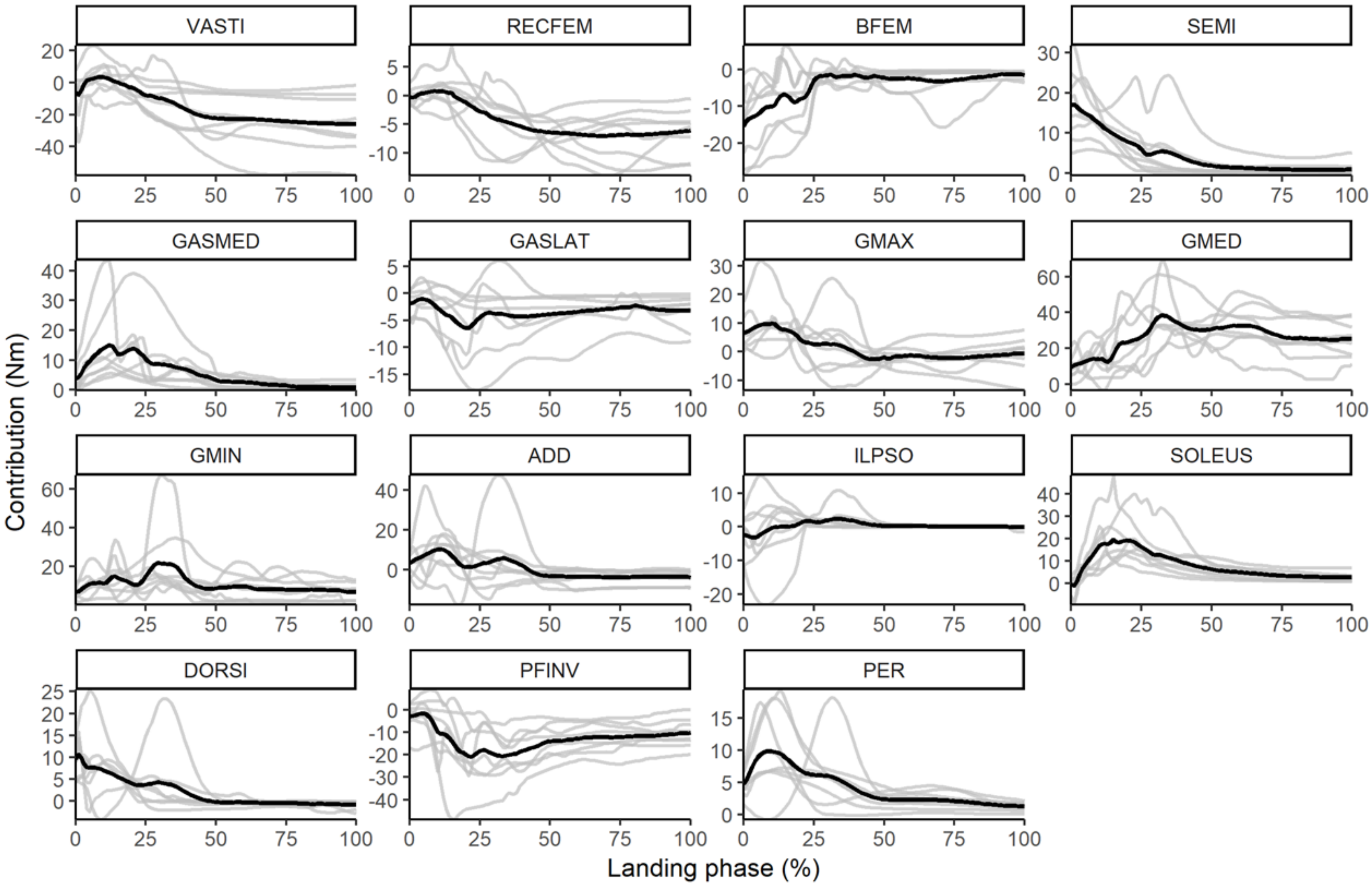
VASTI
RECFEM
BFEM
SEMI
GASMED
GASLAT
GMAX
GMED
GMIN
ADD
ILPSO
SOLEUS
DORSI
PFINV
PER
Contribution (Nm)
Landing phase (%)

725

Supplementary Figure 8. Mean (black line) and individual participant (grey line) contributions of muscles to knee varus/valgus rotation reaction moment for the landing phase (initial contact to peak knee flexion) of a single leg drop landing task from a 0.31m height. Positive values indicate varus moment. RECFEM, rectus femoris; VASTI, vasti (vastus intermedius, lateralis and medialis); GASLAT, gastrocnemius lateralis; GASMED, gastrocnemius medialis; BFEM, biceps femoris (biceps femoris long head and short head), SEMI, medial hamstrings (semitendinosus and semimembranosus); SOLEUS, soleus; PFINV, plantar-flexor-invertors (tibialis posterior, flexor digitorum longus and flexor hallucis longus); PER, peroneus (peroneus brevis and longus); GMAX, gluteus maximus; GMED, gluteus medius; GMIN, gluteus minimus; ILPSO, iliopsoas (iliacus and psoas major); ADD, adductors (adductor brevis, longus and magnus); DORSI, dorsiflexors (tibialis anterior, extensor digitorum and hallucis longus).

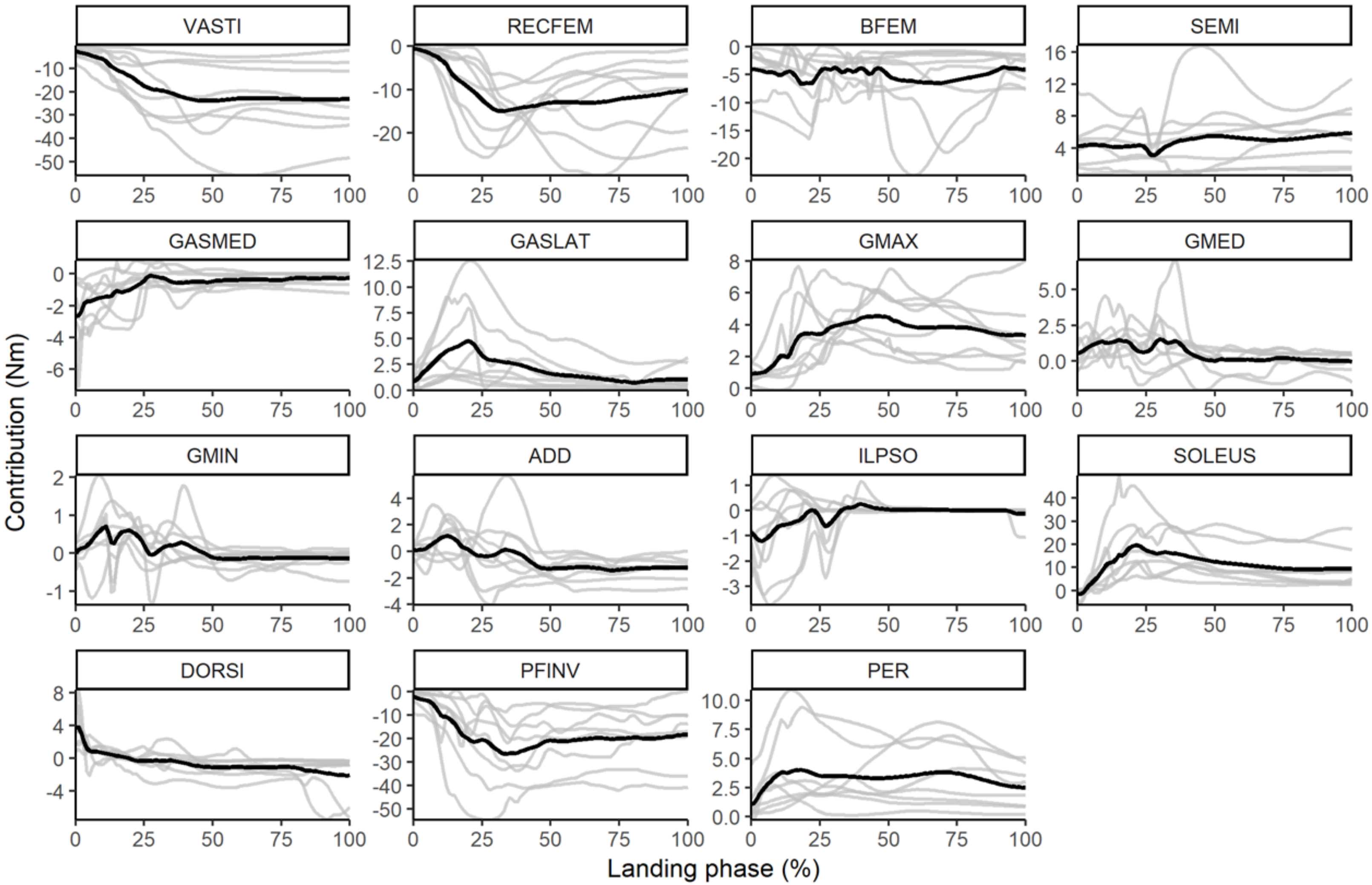
VASTI
RECFEM
BFEM
SEMI
GASMED
GASLAT
GMAX
GMED
GMIN
ADD
ILPSO
SOLEUS
DORSI
PFINV
PER
Contribution (Nm)
Landing phase (%)

Supplementary Figure 9. Mean (black line) and individual participant (grey line) contributions of muscles to knee internal/external rotation reaction moment for the landing phase (initial contact to peak knee flexion) of a single leg drop landing task from a 0.31m height. Positive values indicate internal rotation moment. RECFEM, rectus femoris; VASTI, vasti (vastus intermedius, lateralis and medialis); GASLAT, gastrocnemius lateralis; GASMED, gastrocnemius medialis; BFEM, biceps femoris (biceps femoris long head and short head), SEMI, medial hamstrings (semitendinosus and semimembranosus); SOLEUS, soleus; PFINV, plantar-flexor-invertors (tibialis posterior, flexor digitorum longus and flexor hallucis longus); PER, peroneus (peroneus brevis and longus); GMAX, gluteus maximus; GMED, gluteus medius; GMIN, gluteus minimus; ILPSO, iliopsoas (iliacus and psoas major); ADD, adductors (adductor brevis, longus and magnus); DORSI, dorsiflexors (tibialis anterior, extensor digitorum and hallucis longus).

Supplementary Table 1. Mapping of lower-limb muscles, corresponding model actuators and excitation inputs.

Abbreviation	Muscle group	Muscles	Model actuator	Excitation input
ADD	Adductors	Adductor brevis	addbrev	Synthesised
		Adductor longus	addlong	Synthesised
		Adductor magnus	addmagDist	Synthesised
			addmagIsch	Synthesised
			addmagMid	Synthesised
			addmagProx	Synthesised
BFEM	Biceps femoris	Biceps femoris long head	bflh	EMG (Lateral hamstring)
		Biceps femoris short head	bfsh	Synthesised
DORSI	Dorsiflexors	Extensor digitorum longus	edl	Synthesised
		Extensor hallucis longus	ehl	Synthesised
		Tibialis anterior	tibant	EMG (Tibialis anterior)
GASLAT	Lateral gastrocnemius	Lateral gastrocnemius	gaslat	EMG (Lateral gastrocnemius)
GASMED	Medial gastrocnemius	Medial gastrocnemius	gasmed	EMG (Medial gastrocnemius)
GMAX	Gluteus maximus	Gluteus maximus	glmax1	Synthesised

			glmax2	Synthesised
			glmax3	Synthesised
GMED	Gluteus medius	Gluteus medius	glmed1	Synthesised
			glmed2	Synthesised
			glmed3	Synthesised
GMIN	Gluteus minimus	Gluteus minimus	glmin1	Synthesised
			glmin2	Synthesised
			glmin3	Synthesised
ILPSO	Iliopsoas	Iliacus	iliacus	Synthesised
		Psoas major	psoas	Synthesised
SEMI	Medial hamstrings	Semimembranosus	semimem	EMG (Medial hamstring)
		Semitendinosus	semiten	EMG (Medial hamstring)
PER	Peroneals	Peroneus brevis	perbrev	EMG (Peroneus longus)
		Peroneus longus	perlong	EMG (Peroneus longus)
PFINV	Plantar-flexor-invertors	Flexor digitorum longus	fdl	Synthesised
		Flexor hallucis longus	fhl	Synthesised

		Tibialis posterior	tibpost	Synthesised
RECFEM	Rectus femoris	Rectus femoris	recfem	EMG (Rectus femoris)
SOLEUS	Soleus	Soleus	soleus	EMG (Soleus)
VASTI	Vasti	Vastus intermedius	vasint	EMG (Vastus lateralis)
		Vastus lateralis	vaslat	EMG (Vastus lateralis)
		Vastus medials	vasmed	EMG (Vastus medialis)

EMG, excitations were derived from collected surface electromyography data; Synthesised, excitations were derived from a static optimisation algorithm.

References

1. Hollville E, Nordez A, Guilhem G, Lecompte J, Rabita G. Interactions between fascicles and tendinous tissues in gastrocnemius medialis and vastus lateralis during drop landing. *Scandinavian journal of medicine & science in sports.* 2019;29(1):55-70.
2. Navacchia A, Ueno R, Ford KR, DiCesare CA, Myer GD, Hewett TE. EMG-Informed Musculoskeletal Modeling to Estimate Realistic Knee Anterior Shear Force During Drop Vertical Jump in Female Athletes. *Annals of Biomedical Engineering.* 2019;47(12):2416-2430.